CHAPTER FOUR

SALEN-SUPPORTED, COBALT CATALYSTS FOR CYCLOHEXENE OXIDE/CO_2 COPOLYMERIZATION: SYNTHESIS AND CHARACTERIZATION OF SYNDIOTACTIC POLY(CYCLOHEXENE CARBONATE)

Reprinted in part with permission from

Dalton Transactions **2006**, *1*, 237 – 249.

4.1 Introduction

The correlation between a polymer's main-chain stereochemistry and its physical properties has stimulated many research efforts in the field of stereospecific polymerization. Ordered polymer architectures, where sequential stereocenters are of the same (isotactic) or alternating (syndiotactic) relative configuration are generally more crystalline than their atactic counterparts.[1] Although heterogeneous catalysts can be used to control polymer microstructure in some cases,[2] homogeneous systems are more commonly employed for this purpose.

The alternating copolymerization of cyclohexene oxide (CHO) and CO_2 to generate poly(cyclohexene carbonate) (PCHC) has been a subject of much interest as CO_2 is a readily available, inexpensive, non-toxic, and nonflammable reagent (Scheme 4.1).[3] The asymmetric alternating copolymerization of CHO and CO_2 has been demonstrated first by Nozaki using $ZnEt_2$/chiral amino alcohol catalysts and later by our group using hybrid imine-oxazoline zinc-based catalysts (Figure 4.1).[4-8] In each case, isotactic PCHC with an enantiomeric excess (*ee*) >70% is obtained. These isotactic PCHCs have been structurally characterized by $^{13}C\{^1H\}$ NMR spectroscopy using both model compounds and statistical methods.[6, 9] These systems show that chiral ligands allow the generation of isotactic PCHC, consistent with a site-control copolymerization mechanism (Chapter 2, Scheme 2.3).[4-7]

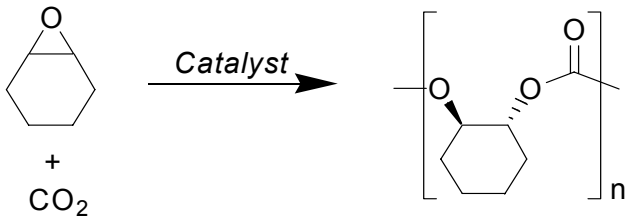

Scheme 4.1. Copolymerization of CHO and CO_2 to yield PCHC.

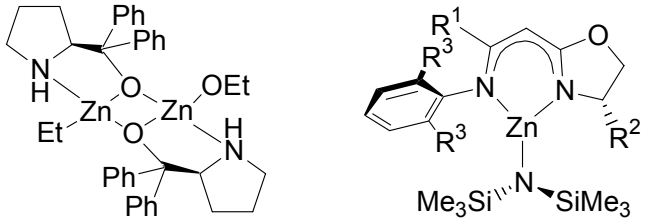

Figure 4.1. Catalysts for the isospecific copolymerization of CHO and CO_2; R^1 = Me, CF_3, or ^{i}Pr; R^2 = (*R*)-Ph, (*S*)-^{i}Pr, or (*S*)-^{t}Bu; R^3 = Et or ^{i}Pr.

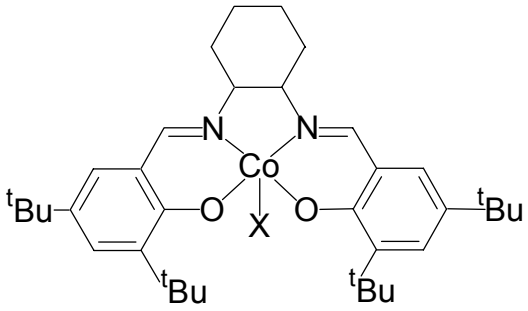

Figure 4.2. (Salen-**1**)CoX catalysts for epoxide/CO_2 copolymerization (X = Cl, Br, I, OAc, pentafluorobenzoate).

As described in Chapters 2 and 3, salen-supported cobalt complexes (Figure 4.2) are highly active catalysts for PO/CO_2 copolymerization to yield PPC with no detectable PC.[10-12] Using these catalyst systems, we observed a variety of PPC microstructures, in which the regio- and stereochemical composition of the PPC formed was dependant on the relative stereochemistry of the catalyst and monomer. Furthermore, through the addition of bulky organic-based, ionic cocatalysts to these systems unprecedented activities were observed, while maintaining excellent regioselectivity. Based on our success with (salen)CoX (X = halide or carboxylate) catalysts for PO/CO_2 copolymerization, we likewise applied these systems to CHO/CO_2 copolymerization, with a focus on maximization of catalyst activity and control of PCHC microstructure.

Herein, we report the synthesis of a series of (salen)CoX complexes that are active for CHO/CO_2 copolymerization. In addition, we address the effects of the salen ligand and catalyst axial ligand/initiator (X) used, the reaction conditions, and the inclusion of [PPN]Cl cocatalysts on activity and stereoselectivity. With these catalysts, we obtain PCHC with various stereochemical architectures, including syndiotactic PCHC, a previously unreported PCHC microstructure. Using Bernoullian statistical methods, we assign PCHC tetrad and triad sequences in the $^{13}C\{^1H\}$ NMR spectra of these polymers in the carbonyl and methylene regions, respectively.

4.2 Catalyst axial ligand (X)

The high PO/CO_2 copolymerization activities and selectivities observed with catalysts (*R,R*)-(salen-**1**)CoX (X = Cl (**2.4**), Br (**2.5**), I (**2.2**), OAc (**2.1**), $OBzF_5$ (**2.3**)) led us to investigate these systems for CHO/CO_2 copolymerization. Initially, we employed high CO_2 pressures (800 psi) with a [CHO]:[Co] loading of 500:1 using a series of catalyst axial ligands/initiators (X). Although the ^1H NMR spectra of the polymers formed were consistent with previously characterized PCHC (Figure 4.3),[13,

[14] the $^{13}C\{^{1}H\}$ NMR spectra were unlike those reported. Based on prior PCHC $^{13}C\{^{1}H\}$ NMR assignments of the carbonyl region,[4, 6, 9] the PCHCs synthesized with catalysts (*R,R*)-(salen-**1**)CoX revealed a strong contribution correlating to *r*-centered tetrads, indicative of *syndiotactic* PCHC (Figure 4.4 and see following discussion).[a] Furthermore, we detected up to 81% *r*-centered tetrads in these PCHCs depending on the catalyst axial ligand/initiator employed. To the best of our knowledge, these are the first CHO/CO_2 copolymerization catalysts to produce syndiotactic PCHC.

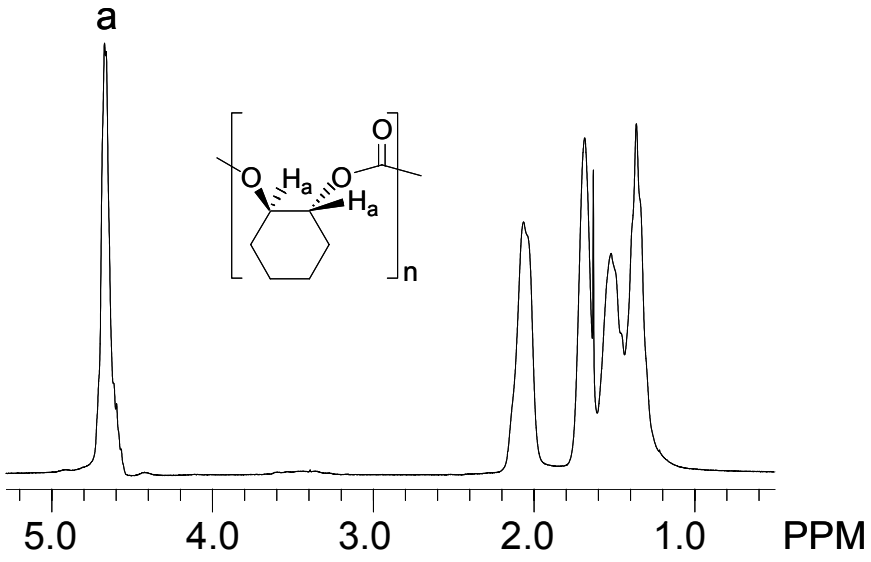

Figure 4.3. ^{1}H NMR ($CDCl_3$, 300 MHz) of syndio-enriched PCHC synthesized using catalyst (*R,R*)-(salen-**1**)CoI (**2.2**).

[a] Quantitative $^{13}C\{^{1}H\}$ NMR spectra of PCHC were deconvoluted prior to integration in order to subtract out the [*rmr*] resonance from the remaining resonances in the 153.2 -152.9 ppm regime. This provided for an approximation of the % *r*-centered tetrads in the PCHC.

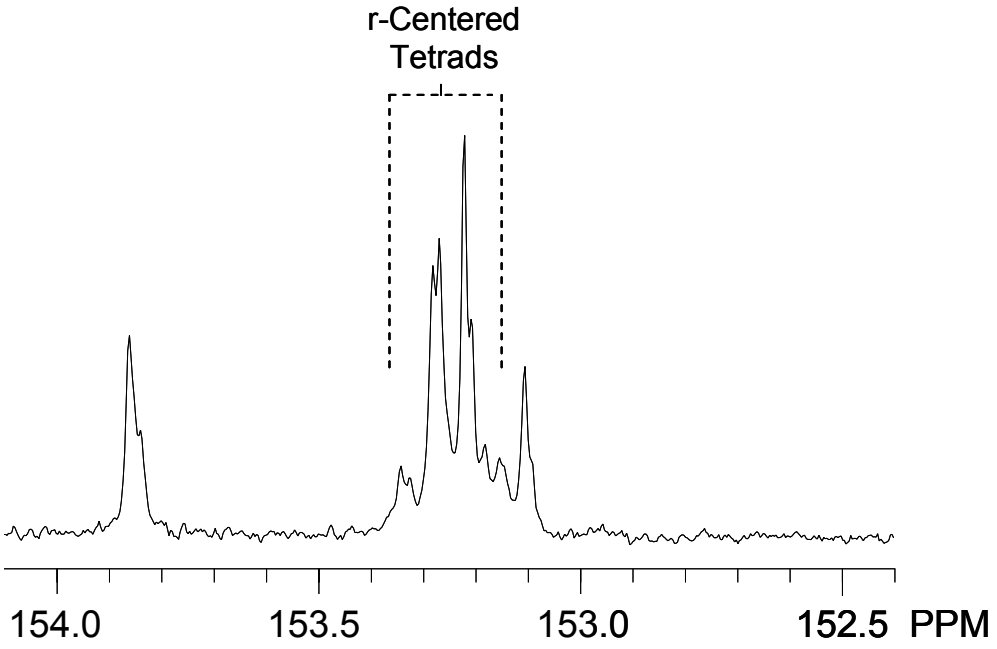

Figure 4.4. Carbonyl region of the quantitative $^{13}C\{^1H\}$ NMR spectrum ($CDCl_3$, 125 MHz, d_1 = 10s) of syndio-enriched PCHC generated using catalyst (*R,R*)-(salen-**1**)CoI (**2.2**).

Table 4.1. Effect of initiator: (*R,R*)-(salen-**1**)CoX catalyzed CHO/CO_2 copolymerization (X = OAc (**2.1**), I (**2.2**), pentafluorobenzoate (**2.3**), Cl (**2.4**), Br (**2.5**)).[a]

Entry	Catalyst	PCHC Yield[b] (%)	TOF[c] (h^{-1})	M_n[d] (kg/mol)	M_w/M_n[d]	*r*-Centered Tetrads[e] (%)
1	**2.1**	27	7	9.8	1.28	64
2	**2.2**	51	13	17.3	1.30	75
3	**2.3**	53	13	16.4	1.30	66
4	**2.4**	62	15	19.7	1.27	68
5	**2.5**	66	16	20.3	1.23	66

[a] Copolymerizations neat at 22 °C for 20 h at 800 psi of CO_2 with [CHO]:[Co] = 500:1. In all cases, cyclohexene carbonate is not observed and PCHCs have ≥ 96% carbonate linkages as determined by ^1H NMR spectroscopy ($CDCl_3$, 300 MHz). [b] Based on isolated PCHC yield. [c] Turnover frequency for PCHC = (mol CHO/(mol Co · h)). [d] Determined by GPC calibrated with polystyrene standards in THF at 40 °C. [e] Determined by quantitative $^{13}C\{^1H\}$ NMR spectroscopy ($CDCl_3$, 125 MHz, d_1 = 10s).

The CHO/CO_2 copolymerization data for **2.1** - **2.5** catalysts are listed in Table 4.1. While most of the catalyst activities were quite similar (entries 2 - 5), when acetate was used as an initiating group, catalyst activity decreases substantially (entry 1). Overall, (*R,R*)-(salen-**1**)CoX catalysts had TOFs $\leq$ 16 h^{-1} for CHO/CO_2 copolymerization. As much higher activities were observed with these catalyst systems for PO/CO_2 copolymerization under comparable reaction conditions, we suspect that reaction rates are hindered by the more sterically bulky, less reactive CHO monomer. Generally, variation of the axial ligand/initiator had little influence on the syndiotacticity of the resultant PCHC, however, when iodide was used, the resultant PCHC was exceptionally syndiotactic. Furthermore, the role of the iodide axial ligand in the CHO/CO_2 copolymerization is under current investigation.

In all cases, the PCHCs we obtained exhibit M_n values lower than the corresponding theoretical values despite the absence of chain transfer agents. Notably, this was not observed with these catalyst systems for PO/CO_2 copolymerization under comparable reaction conditions, and may be attributable to chain transfer to monomer or trace water and/or the formation of cyclic polymer (Scheme 2.4 and Scheme 3.1).

4.3 Salen ligand: backbone structure

It has been shown previously that minor alterations of the salen ligands in their chromium-, cobalt- or aluminum-based complexes have dramatic effects on epoxide/CO_2 copolymerization activity.[15-18] To explore the relationship of the structural features of the salen ligand to catalyst performance in our systems, we prepared a diverse series of salen ligands (Figure 4.5) for use in the synthesis of CHO/CO_2 copolymerization catalysts. It is notable that the axial ligand Br was used, as the analogous I complexes proved too difficult to purify by the filtration methods used.

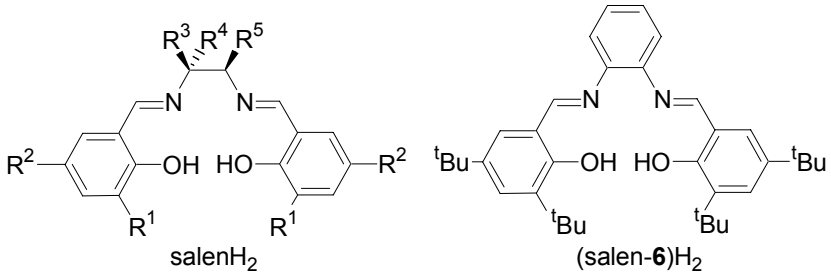

salenH_2 (salen-**6**)H_2 (**2.12**)

Ligand		R^1	R^2	R^3	R^4	R^5
(*R,R*)-(salen-**1**)H_2	(**2.6**)	^{t}Bu	^{t}Bu	H	*trans*-(*R,R*)	-$(CH_2)_4$-
rac-(salen-**1**)H_2	(**2.7**)	^{t}Bu	^{t}Bu	H	*trans*-(*R,R*)	-$(CH_2)_4$-
rac-(salen-**2**)H_2	(**4.1**)	^{t}Bu	^{t}Bu	Me	H	H
(salen-**3**)H_2	(**2.9**)	^{t}Bu	^{t}Bu	H	H	H
(salen-**4**)H_2	(**2.10**)	^{t}Bu	^{t}Bu	Me	Me	H
(*R,R*)-(salen-**5**)H_2	(**2.11**)	^{t}Bu	^{t}Bu	H	(*R*)-Ph	*trans*-(*R*)-Ph
(*R,R*)-(salen-**11**)H_2	(**2.17**)	cumyl	cumyl	H	*trans*-(*R,R*)	-$(CH_2)_4$-
rac-(salen-**12**)H_2	(**4.2**)	cumyl	cumyl	Me	H	H
rac-(salen-**13**)H_2	(**4.3**)	Me	H	Me	H	H
rac-(salen-**14**)H_2	(**4.4**)	^{t}Bu	H	Me	H	H
rac-(salen-**15**)H_2	(**4.5**)	^{t}Bu	Br	Me	H	H

Figure 4.5. Salen ligands for the synthesis of (salen)CoX CHO/CO_2 copolymerization catalysts. Cumyl = α,α'-dimethylbenzyl.

Table 4.2. Effect of backbone structure on catalyst activity and syndioselectivity: (salen)CoBr catalyzed CHO/CO_2 copolymerization.[a]

Entry	Catalyst	Time (h)	PCHC Yield[b] (%)	TOF[c] (h^{-1})	M_n[d] (kg/mol)	M_w/M_n[d]	*r*-Centered Tetrads[e] (%)
1	(*R,R*)-(salen-**1**)CoBr (**2.5**)	20	66	16	20.3	1.23	66
2	*rac*-(salen-**1**)CoBr (**2.30**)	20	64	16	23.7	1.22	78
3	(*R,R*)-(salen-**5**)CoBr (**2.22**)	20	8	2	7.7	1.46	61
4	(salen-**6**)CoBr (**2.23**)	20	<1	NA	NA	NA	NA
5	(salen-**4**)CoBr (**2.19**)	20	35	9	14.2	1.35	75
6	(salen-**3**)CoBr (**2.20**)	20	90	22	26.3	1.24	75
7	*rac*-(salen-**2**)CoBr (**4.6**)	20	87	22	30.3	1.28	80
8	**4.6**	3	59	98	21.0	1.32	81

[a] Copolymerizations run neat at 22 °C with [CHO]:[Co] = 500:1 at 800 psi of CO_2. In all cases, cyclohexene carbonate is not observed and PCHCs have ≥ 96% carbonate linkages as determined by ^{1}H NMR spectroscopy ($CDCl_3$, 300 MHz). [b] Based on isolated PCHC yield. [c] Turnover frequency for PCHC = (mol CHO/(mol Co · h)). [d] Determined by GPC calibrated with polystyrene standards in THF at 40 °C. [e] Determined by quantitative $^{13}C\{^1H\}$ NMR spectroscopy ($CDCl_3$, 125 MHz, d_1 = 10s).

Table 4.2 lists the CHO/CO_2 copolymerization data for a series of (salen)CoBr catalysts, in which systematic changes in the diimine backbone have been employed. In all cases a [CHO]:[Co] loading of 500:1 was applied while using high CO_2 pressures (800 psi). Catalyst **2.5** produces PCHC with 66% *r*-centered tetrads and a TOF of 16 h^{-1} (entry 1). Alternatively, its racemic analogue (**2.30**) is more syndioselective, generating PCHC with 78% *r*-centered tetrads (entry 2). Increasing the steric bulk on the catalyst backbone ((*R,R*)-(salen-**5**)CoBr (**2.22**)) reduces the TOF to 2 h^{-1} and yields PCHC with only 61% *r*-centered tetrads (entry 3). Complex (salen-**6**)CoBr (**2.23**), with a phenylene diimine backbone, has very low activity for the CHO/CO_2 copolymerization with only trace PCHC observed after 20 h (entry 4). Although the similar complex (salen-**3**)CoOAc is highly active for isospecific PO homopolymerization,[19] **2.23** does not catalyze this transformation. The CHO/CO_2

copolymerization rate is also reduced compared to that observed with **2.5** when a 1,1-dimethyl substituted backbone is used ((salen-**4**)CoBr (**2.19**); entry 5). However, decreasing the steric bulk with (salen-**3**)CoBr (**2.20**) or *rac*-(salen-**2**)CoBr (**4.6**) results in a substantial increase in catalyst activity while maintaining the high syndioselectivity initially observed (entries 6 and 7). In fact, complex **4.6** produces PCHC with 81% *r*-centered tetrads, which is the greatest syndiotacticity that we have observed in PCHC formation to date. Interestingly, use of the most active catalysts (**2.20** or **4.6**) results in very high conversions even though the polymerization is run in neat CHO (entries 6 and 7). We suspect that at 800 psi, CO_2 plays a role as a solvent and/or lowers the viscosity of the reaction mixture such that the polymerization can proceed to high PCHC yields. Finally, based on a shorter reaction time, catalyst **4.6** exhibited the highest activity for these systems (TOF = 98 h^{-1}; entry 8). In general, the highest activity and syndioselectivity were both achieved by using a racemic salen ligand backbone with minimal steric hindrance.

4.4 Salen ligand: phenolate substitution

Using the highly active *rac*-propyldiimine ligand backbone, we investigated the influence of the phenolate *ortho* and *para* substituents on (salen)CoX catalyzed CHO/CO_2 copolymerization (Table 4.3). It is notable that the catalyst axial ligand X = $OBzF_5$ was used in this study (instead of X = Br as above) because the complexes *rac*-(salen-**8**)CoBr and *rac*-(salen-**9**)CoBr proved too soluble to purify by washing with pentane. The CHO/CO_2 copolymerization using catalyst *rac*-(salen-**6**)CoOBzF_5 (**4.7**) is highly active with a TOF of 93 h^{-1} yielding PCHC with 76% *r*-centered tetrads (entry 1). These values are similar to those observed with the analogous X = Br complex (**4.6**) (Table 4.3, entry 8). Increasing the steric bulk of the phenolate *ortho* and *para* substituents using *rac*-(salen-**12**)CoOBzF_5 (**4.8**) is detrimental, decreasing catalyst activity to a TOF of 5 h^{-1} and reducing syndiotacticity to 65% (entry 2).

Alternatively, using catalyst *rac*-(salen-**13**)CoOBzF$_5$ (**4.9**) where the steric bulk of the *ortho* and *para* positions is virtually nonexistent results in a complete loss in stereoselectivity yielding atactic PCHC (entry 3). In the intermediate cases which incorporating *tert*-butyl groups in the *ortho* positions while varying the *para* positions of the phenolate to either H or Br (*rac*-(salen-**14**)CoOBzF$_5$ (**4.10**) or *rac*-(salen-**15**)CoOBzF$_5$ (**4.11**), respectably) catalyst activity and syndioselectivity are decreased (entries 4 and 5). Largely, the salen ligand with *tert*-butyl groups in both the *ortho* and *para* positions of the phenolate moiety provides the ideal steric bulk for use in the CHO/CO_2 copolymerizations, giving high activity and syndioselectivity.

Table 4.3 Effect of phenolate substituents: (salen)CoOBzF$_5$ catalyzed CHO/CO_2 copolymerization.[a]

Entry	Catalyst	Time (h)	PCHC Yield[b] (%)	TOF[c] (h^{-1})	M_n[d] (kg/mol)	M_w/M_n[d]	*r*-Centered Tetrads[e] (%)
1	*rac*-(salen-**2**)CoOBzF$_5$ (**4.7**)	3	56	93	22.3	1.35	76
2	*rac*-(salen-**12**)CoOBzF$_5$ (**4.8**)	20	22	5	11.7	1.40	65
3	*rac*-(salen-**13**)CoOBzF$_5$ (**4.9**)	3	19	32	10.9	1.22	50
4	*rac*-(salen-**14**)CoOBzF$_5$ (**4.10**)	3	39	65	14.5	1.42	66
5[f]	*rac*-(salen-**15**)CoOBzF$_5$ (**4.11**)	3	30	50	14.6	1.38	75

[a] Copolymerizations run neat at 22 °C with [CHO]:[Co] = 500:1 at 800 psi of CO_2. In all cases, cyclohexene carbonate is not observed and PCHCs have ≥ 96% carbonate linkages as determined by ^{1}H NMR spectroscopy ($CDCl_3$, 300 MHz). [b] Based on isolated PCHC yield. [c] Turnover frequency for PCHC = (mol CHO/(mol Co · h)). [d] Determined by GPC calibrated with polystyrene standards in THF at 40 °C. [e] Determined by quantitative $^{13}C\{^1H\}$ NMR spectroscopy ($CDCl_3$, 125 MHz, d_1 = 10s). [f] 93% carbonate linkages.

As enantiomerically pure, racemic, and achiral (salen)CoX catalysts are all syndioselective for CHO/CO_2 copolymerization, we suspect that monomer enchainment proceeds by a chain-end control mechanism where the stereogenic center from the last enchained monomer unit influences the stereochemical outcome of subsequent monomer addition (Chapter 2, Scheme 2.3). Notably, this propagation scheme becomes competitive with an enantiomorphic-site control pathway in the case of some (salen)CoX catalysts, resulting in a loss of syndioselectivity. Based on the results presented above, we believe that an enantiomorphic-site control mechanism is competitive for (salen)CoX catalysts with a sterically bulky diimine backbone or cumyl *ortho* and *para* phenolate substituents. Also, in the case of catalyst **4.14**, where the steric bulk of the salen ligand is minimal, all stereochemical direction is lost, showing that moderate ligand steric bulk is necessary for chain-end control. Overall, the optimized ligand structure for maximum catalyst activity and syndioselectivity is achieved with minimal steric bulk on the salen diimine backbone and *tert*-butyl moieties present in the *ortho* and *para* positions of the phenolate.

4.5 CO_2 pressure

In an effort to investigate the relationship between PCHC tacticity and the applied CO_2 pressure, we proceeded to explore a series of (salen)CoX catalysts for the CHO/CO_2 copolymerization at low CO_2 pressures (100 psi) at 22 °C (Table 4.4). In all cases, catalyst activity decreased notably, and reaction times were increased to 48 h or longer in order to achieve appreciable conversion. In addition, the CHO/CO_2 copolymerizations at low CO_2 pressures generally resulted in a loss of syndioselectivity and decreased carbonate incorporation in the resultant PCHC. Catalyst **2.5** showed no syndioselectivity yielding atactic PCHC with only 90% carbonate incorporation (entry 1). Using our most sterically bulky complex (*R,R*)-(salen-**11**)CoBr (**2.29**), however, surprising produced *isoenriched* PCHC with 65% *m*-

centered tetrads and 99% carbonate incorporation (entry 2). When this PCHC was broken down to cyclohexane diol while maintaining all stereocenters, we observed an (*R,R*) to (*S,S*) ratio of 78:22 as determined by GC. Interestingly, the sterically bulky catalyst **2.22** incorporated very little CO_2, producing predominantly poly(cyclohexene oxide) (entry 3). One of our best catalysts at high pressure (**4.7**) showed a decrease in syndioselectivity with CO_2 at 100 psi generating PCHC with only 60% *r*-centered tetrads and 88% carbonate linkages (entry 4), whereas changing the axial ligand to Br (**4.6**) completely eliminated any syndioselectivity (entry 5).

Table 4.4 Effect of catalyst structure: (salen)CoX catalyzed CHO/CO_2 copolymerization at low CO_2 pressures (X = Br, $OBzF_5$).[a]

Entry	Catalyst		Time (h)	PCHC Yield[b] (%)	TOF[c] (h^{-1})	Carbonate Linkages (%)[d]	M_n[e] (kg/mol)	M_w/M_n[e]	*r*-Centered Tetrads[f] (%)
1	(*R,R*)-(salen-**1**)CoBr	(**2.5**)	48	35	4	90	12.6	1.23	50
2	(*R,R*)-(salen-**11**)CoBr	(**2.29**)	72	32	2	99	8.9	1.19	35
3	(*R,R*)-(salen-**5**)CoBr	(**2.22**)	72	10	<1	20	10.8	1.83	NA
4	*rac*-(salen-**2**)CoOBzF_5	(**4.7**)	48	35	4	88	9.3	1.27	60
5	*rac*-(salen-**2**)CoBr	(**4.6**)	72	17	1	86	6.5	1.33	51

[a] Copolymerizations run neat at 22 °C with [CHO]:[Co] = 500:1 at 100 psi of CO_2. In all cases, cyclohexene carbonate is not observed. [b] Based on isolated PCHC yield. [c] Turnover frequency for PCHC = (mol CHO/(mol Co · h)). [d] Determined by ^1H NMR spectroscopy ($CDCl_3$, 300 MHz). [e] Determined by GPC calibrated with polystyrene standards in THF at 40 °C. [f] Determined by quantitative $^{13}C\{^1H\}$ NMR spectroscopy ($CDCl_3$, 125 MHz, d_1 = 10s).

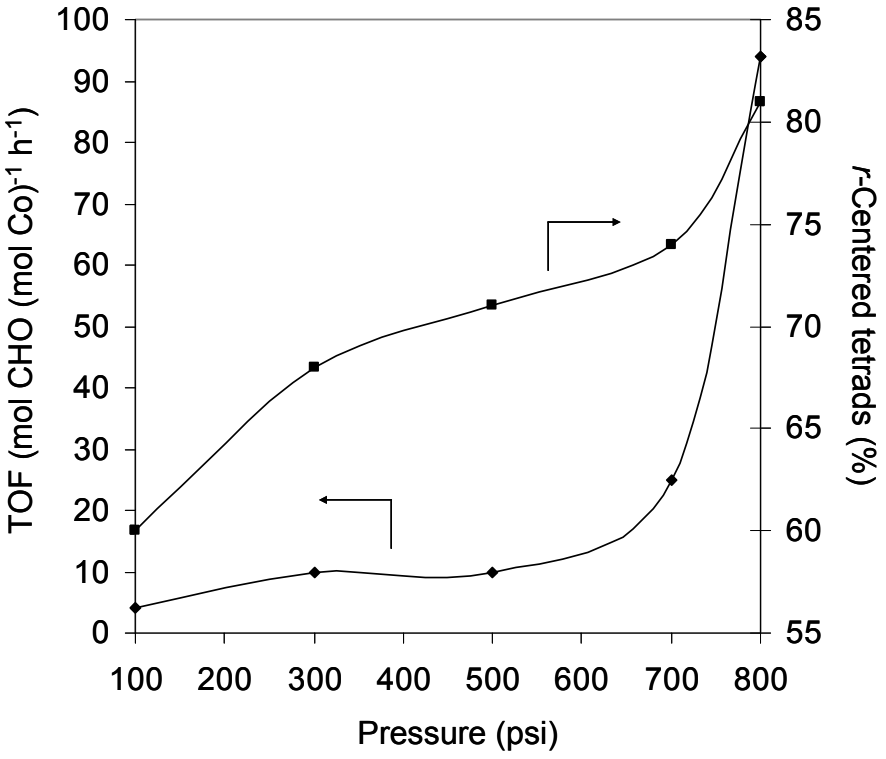

Figure 4.6. The effect of CO_2 pressure on catalyst activity and syndioselectivity for CHO/CO_2 copolymerization with *rac*-(salen-**2**)CoOBzF_5 (**4.7**).

To further correlate CO_2 pressure to catalyst activity and syndioselectivity, we continued to investigate the CHO/CO_2 copolymerization using **4.7** at a series of different CO_2 pressures. Results from these experiments are presented graphically in Figure 4.6. It is notable that 800 psi is the highest pressure we are able to obtain at 22 °C using our standard copolymerization setup and was therefore the highest pressure applied. Decreasing the CO_2 pressure from 800 psi to 700 psi caused a dramatic loss in catalyst activity, consistent with the results we observe with (salen)CoX catalysts for PO/CO_2 copolymerization. Further reductions in CO_2 pressure resulted in a slow but steady decrease in catalyst activity. The syndioselectivity of catalyst **4.7** is optimized at 800 psi of CO_2 at 22 °C, and parallels the catalyst activity at all pressures employed.

4.6 Addition of [PPN]Cl cocatalysts

Previous investigations have shown that the addition of organic-based, ionic cocatalysts to porphyrin- or salen-supported catalysts for epoxide/CO_2 copolymerization often leads to increased reaction rates.[12, 15, 20-26] In our earlier work, addition of [PPN]Cl to **2.3** for PO/CO_2 copolymerization led to a dramatic increase in reaction rate as compared with the use of **2.3** alone. In addition, **2.3**/[PPN]Cl was most active for PO/CO_2 copolymerization at *low* CO_2 pressures, which has allowed the development of optimized systems functioning under only 100 psi of CO_2. Based on these findings, we describe the effect of [PPN]Cl in the CHO/CO_2 copolymerization using a series of (salen)CoX (X = Br, $OBzF_5$) catalysts under various reaction conditions (Table 4.5).

We initially applied [PPN]Cl cocatalysts to the (salen)CoX catalyzed CHO/CO_2 copolymerization at high CO_2 pressures in an effort to maximize catalyst syndioselectivity. Interestingly, catalyst system **2.5**/[PPN]Cl showed a loss in syndioselectivity from use of **2.5** alone. Additionally, only a small increase in activity was observed upon the addition of the [PPN]Cl cocatalyst. By varying the catalyst axial ligand in (*R,R*)-(salen-**1**)CoX/[PPN]Cl from Br (**2.5**) to $OBzF_5$ (**2.3**) we observe little change in activity and syndioselectivity (entries 1 and 2). Surprisingly, catalyst **4.7**, one of the fastest catalysts without an additive, was less active for CHO/CO_2 copolymerization upon the inclusion of [PPN]Cl (entry 3). Similar to the (*R,R*)-(salen)CoX/[PPN]Cl (X = Br (**2.5**), $OBzF_5$ (**2.3**)) catalyst systems, little syndioselectivity was realized in this case.

Table 4.5. Effect of [PPN]Cl cocatalyst: (salen)CoX/[PPN]Cl catalyzed CHO/CO_2 copolymerization (X = Br, pentafluorobenzoate ($OBzF_5$)).[a]

Entry	Catalyst	CO_2 Pressure (psi)	Time (h)	PCHC Yield[b] (%)	TOF[c] (h^{-1})	M_n[d] (kg/mol)	M_w/M_n[d]	*r*-Centered Tetrads[e] (%)
1	(*R,R*)-(salen-**1**)CoBr (**2.5**)	800	6	34	57	14.8	1.38	62
2	(*R,R*)-(salen-**1**)CoOBzF$_5$ (**2.3**)	800	6	40	67	15.0	1.36	59
3	*rac*-(salen-**2**)CoOBzF$_5$ (**4.7**)	800	6	18	30	10.1	1.44	62
4	(*R,R*)-(salen-**5**)CoOBzF$_5$ (**3.5**)	800	6	36	60	11.8	1.38	50
5	(*R,R*)-(salen-**11**)CoOBzF$_5$ (**3.7**)	800	6	27	45	10.6	1.41	51
6	**2.5**	100	2	22	110	8.2	1.24	47
7	**2.3**	100	2	32	160	14.9	1.14	49
8	**4.7**	100	2	18	90	7.4	1.22	56
9	**3.5**	100	2	13	65	6.6	1.18	42
10	**3.7**	100	14	44	31	15.3	1.17	44
11[f]	**2.3**	100	1	44	440	11.9	1.23	47

[a] Copolymerizations run neat at 22 °C with [CHO]:[Co]:[[PPN]Cl] = 1000:1:1. In all cases, cyclohexene carbonate is not observed and PCHCs have ≥ 97% carbonate linkages as determined by ^{1}H NMR spectroscopy ($CDCl_3$, 300 MHz). [b] Based on isolated PCHC yield. [c] Turnover frequency for PCHC = (mol CHO/(mol Co · h)) [d] Determined by GPC calibrated with polystyrene standards in THF at 40 °C. [e] Determined by quantitative $^{13}C\{^1H\}$ NMR spectroscopy ($CDCl_3$, 125 MHz, d_1 = 10s). [f] 70 °C.

The loss of syndioselectivity upon the addition of [PPN]Cl to the (salen)CoX catalyzed CHO/CO_2 copolymerization indicates that a chain-end control mechanism exerts less control on the stereoselectivity of the polymerization. We therefore explored (salen)CoOBzF_5 catalysts with sterically bulky salen ligands in an effort to invoke a site-control mechanism for isotactic PCHC. Application of (*R,R*)-(salen-**5**)CoOBzF_5 (**3.5**)/[PPN]Cl, with a more sterically bulky diimine backbone, had comparable activity to **2.3**/[PPN]Cl however the resultant PCHC was atactic (entry 4). Additionally, employing a more sterically bulky phenolate moiety ((*R,R*)-(salen-**11**)CoOBzF_5 (**3.7**)/[PPN]Cl) also generated atactic PCHC with slightly lower activity (entry 5). In general, addition of [PPN]Cl cocatalysts to (salen)CoX catalyzed CHO/CO_2 copolymerization at high CO_2 pressures results in a loss in stereoselectivity with little or no increase in activity.

At low CO_2 pressures (100 psi), catalyst activities increase dramatically upon the addition of [PPN]Cl to the copolymerization, although product PCHCs become virtually atactic. Catalyst systems (*R,R*)-(salen-**1**)CoX/[PPN]Cl (X = Br (**2.5**), OBzF_5 (**2.3**)) are highly active with TOFs of 110 h^{-1} and 160 h^{-1}, respectively, producing atactic PCHC (entries 6 and 7). **4.7**/[PPN]Cl was less active for CHO/CO_2 copolymerization with a TOF of 90 h^{-1} (entry 8), while use of the more sterically bulky **3.5**/[PPN]Cl or **3.7**/[PPN]Cl resulted in even lower TOFs of 65 h^{-1} and 31 h^{-1} (entries 9 and 10). Overall, when using the cocatalyst [PPN]Cl, **2.3** is the most active catalyst for CHO/CO_2 copolymerization at low CO_2 pressures.

Although use of elevated temperatures for **2.3**/[PPN]Cl catalyzed PO/CO_2 copolymerization predominantly forms PC, we did not observe the analogous cyclohexene carbonate upon heating the CHO/CO_2 copolymerization. Furthermore, at the optimized temperature of 70 °C, catalyst system **2.3**/[PPN]Cl generates PCHC with a TOF of 440 h^{-1} (entry 11). Notably, this is the fastest catalyst activity we

observe with the (salen)CoX/[PPN]Cl systems, although inferior to zinc- and chromium-based alternatives.[3]

4.7 Stereochemical assignment of PCHC

In previous accounts, stereoregular PCHC has been classified according to the relative stereochemistry of the carbons on the cyclohexane units at which the main chain enters (Figure 4.7).[6, 9] In all reported cases to date, the main chain bonds entering and leaving the enchained cyclohexane units of PCHC are oriented *trans* to each other. Furthermore, although stereoregular PCHC is conventionally a ditactic polymer,[27] assigning the relative stereochemistry for the carbons at which the main chain leaves provides no additional stereochemical information and has therefore been generally omitted (Figure 4.7b). In keeping with the previously established conventions in this field, it is important to note that [*m*] and [*r*] assignments used herein represent the relative stereochemistry of the carbons of the cyclohexane units at which the main chain enters (Figure 4.7a), not the relative stereochemistry of the two carbons on either side of the carbonate unit (Figure 4.7c). Therefore a *racemo* diad, [*r*], represents two entire monomer units that have been incorporated in the opposite stereochemical orientation.

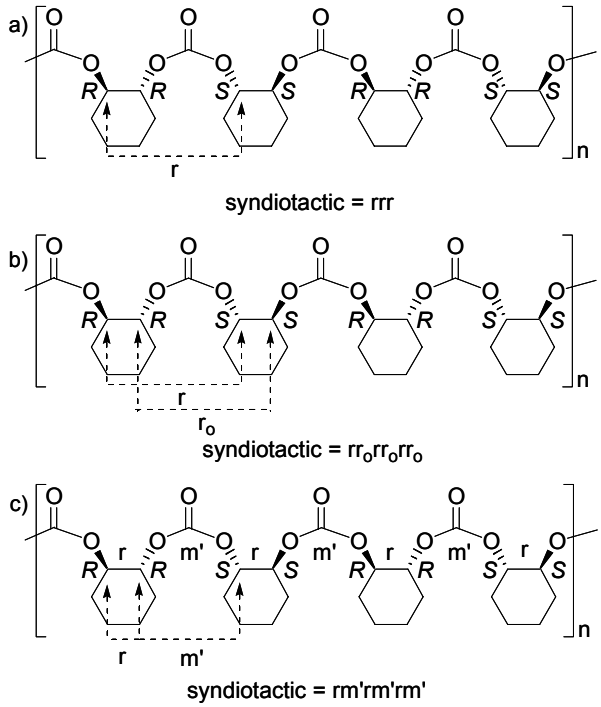

Figure 4.7. Classification of PCHC according to the relative stereochemistry of a) the carbon at which the main chain enters the cyclohexane unit b), the carbon at which the main chain enters and leaves the cyclohexane unit and c) and adjacent carbons.

4.8 Stereochemical characterization and analysis of PCHC

In earlier reports, we and Nozaki assigned the carbonyl region of the $^{13}C\{^1H\}$ NMR spectrum for isotactic PCHC,[4, 6] which was further corroborated using statistical methods.[6] Additionally, Nozaki has assigned the resonances corresponding to [*mmm*] and [*rrr*] tetrad sequences by synthesizing model PCHC oligomers.[9] In each case, all [*mmm*], [*mmr*], and [*rmr*] tetrads were correlated to one central resonance at 153.7 ppm and the remaining *r*-centered tetrads resided in the 153.3 – 153.1 ppm range. Isotactic PCHC was therefore characterized by a strong resonance at 153.7 ppm with a smaller series of resonances from 153.3 – 153.1 ppm due to stereoerrors. Statistically

(enantiomorphic-site control), the most prominent stereoerrors in isotactic PCHC are [*mrm*] and [*mmr*] tetrads, with much smaller contributions from the remaining [*rrr*], [*rmr*], and [*rrm*] tetrads (Figure 4.8). This is a result of isolated stereoerrors that are immediately corrected rather than propagated. In contrast, the PCHC that we obtain with catalyst **4.7** revealed a $^{13}C\{^{1}H\}$ NMR spectrum with four distinct resonances at 152.94, 153.06, 153.12, and 153.70 ppm integrating to 9%, 56%, 24%, and 11%, respectively (Figure 4.9a).[b]

[b] Quantitative $^{13}C\{^{1}H\}$ NMR spectra of PCHC were deconvoluted prior to integration in order to subtract out the [*rmr*] resonance from the remaining resonances in the 153.2 -152.9 ppm regime. This provided for an approximation of the % *r*-centered tetrads in the PCHC.

Syndiotactic Poly(cyclohexene carbonate) (PCHC)

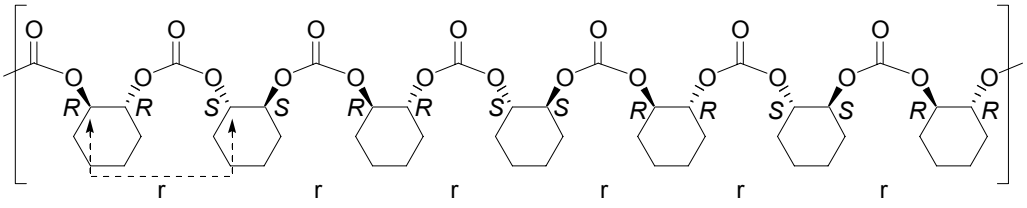

Isolated Stereoerror in Syndiotactic PCHC: Enantiomorphic-Site Control Mechanism

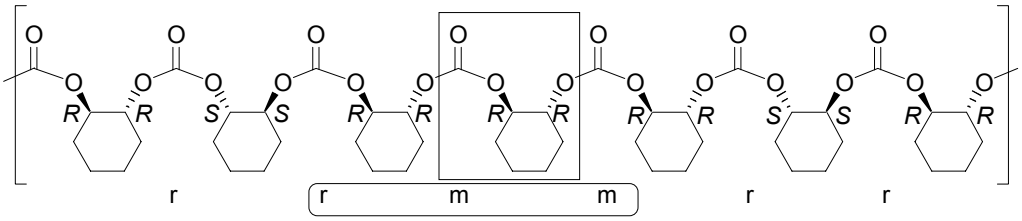

Propagated Stereoerror in Syndiotactic PCHC: Chain-End Control Mechanism

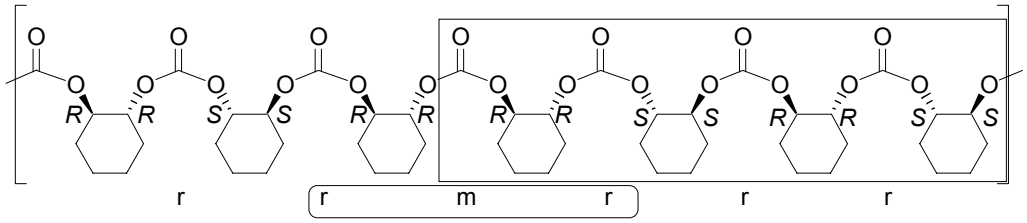

Figure 4.8 Common stereoerrors in syndiotactic PCHC for enantiomorphic-site control and chain-end control propagation mechanisms.

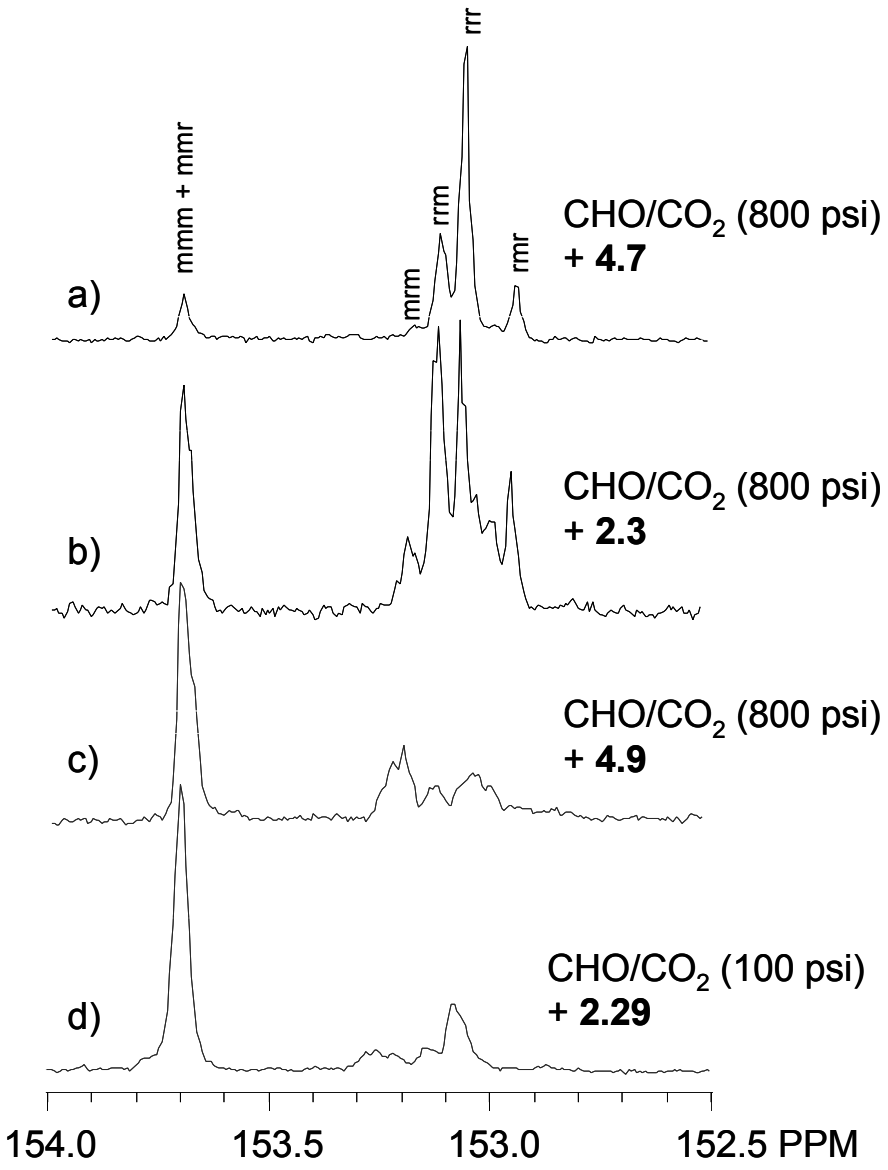

Figure 4.9. Carbonyl region of the quantitative $^{13}C\{^1H\}$ NMR spectra ($CDCl_3$, 125 MHz, d_1 = 10s) of PCHCs generated using CHO/CO_2 (800 psi) with catalyst a) *rac*-(salen-**2**)CoOBzF_5 (**4.7**), b) (*R,R*)-(salen-**1**)CoOBzF_5 (**2.3**), c) *rac*-(salen-**13**)CoOBzF_5 (**4.9**) and d) CHO/CO_2 (100 psi) with catalyst (*R,R*)-(salen-**11**)CoBr (**2.29**).

Table 4.6. Comparison of observed tetrad concentrations to corresponding calculated statistical occurrences in syndiotactic PCHC.[a]

	P_r		[*mmm*]/[*mmr*]		[*rmr*]		[*rrr*]		[*rrm*]	
Table/ Entry	Calc (%)	Obs (%)	Calc (%)	Obs (%)	Calc (%)	Obs (%)	Calc (%)	Obs (%)	Calc (%)	Obs (%)
4.2/7	82	80	6	10	12	12	55	55	24	24
4.3/1	82	76	6	9	12	11	56	56	24	24
4.3/5	81	75	7	11	13	10	53	53	25	26
4.2/2	79	78	8	11	13	11	49	49	26	29
4.2/6	77	75	9	15	14	14	46	46	27	26
4.1/5	71	66	15	25	15	13	35	35	29	26
4.1/2	68	66	17	24	15	16	32	32	30	28
4.3/2	66	65	19	26	15	15	29	29	30	31

[a] Calculated (calc) statistical occurrences for each tetrad were determined through application of Bernoullian (chain-end control) statistical methods where the calculated probability of a racemo diad (P_r) was determined by the maximized weighted fit between calculated and observed (obs) tetrad concentrations. All observed values determined by quantitative $^{13}C\{^1H\}$ NMR spectroscopy ($CDCl_3$, 125 MHz, d_1 =10s) with deconvolution of $^{13}C\{^1H\}$ NMR resonances. In all cases, the [*mrm*] tetrad concentrations (calc values between 2 - 7%) were too small for analysis by the deconvolution methods used and were therefore omitted.

The peak at 152.94 ppm is unique to this polymer and was unobserved in isotactic PCHC.[6, 9] Based on the previous assignments, we correlated the most intense resonance at 153.06 ppm to the [*rrr*] tetrad, with a relative integration of 56%. Using Bernoullian (chain-end control) statistical methods (Scheme 4.2), such that the calculated probability of a racemo diad (P_r) was determined by the maximized weighted fit between calculated and observed (obs) tetrad concentrations[c] we calculate 56% [*rrr*] tetrads, 24% [*rrm*] tetrads and 12% tetrads, with the remaining tetrads: [*mmr*] = 5%, [*mrm*] = 2%, and [*mmm*] = 1% (Table 4.6). The previous reports

[c] The probability of a racemo diad (P_r) was set such that the weighted fit between calculated and observed tetrad concentrations were maximized. The observed tetrad concentrations ([*rrr*], [*rrm*], [*rmr*], and [*rmm*] + [*mmm*]) were determined from quantitative $^{13}C\{^1H\}$ NMR spectroscopy where the resonances in the carbonyl region were deconvoluted prior to integration. The remaining [*mrm*] tetrad was too small for analysis by the deconvolution methods used, and was therefore omitted. The assignment of P_r was based on the minimization of the difference between the observed and calculated tetrad concentrations and was determined by the following: $[rrr]\cdot|[rrr] - P_r^3| + [rmr]\cdot|[rmr] - P_r^2(1 - P_r)| + [mrr]\cdot|[mrr] - 2(P_r^2(1-P_r))| + ([mmm] + [mmr])\cdot|([mmm] + [mmr]) - ((1-P_r)^3 + 2(P_r(1-P_r)^2))|$.

assigning all *m*-centered tetrads to a central resonance at 153.7 ppm do not agree with these statistical calculations. We therefore propose that the [*rmr*] tetrad corresponds to the most upfield resonance at 152.94 ppm in our spectrum, an unobservable stereoerror in isotactic PCHC samples, due to its low probability, leading to a previously incorrect assignment. It is also important to note that the [*rmr*] tetrad was not investigated in previous syntheses of model oligomers,[9] precluding its direct assignment through chemical means. Finally, we attribute the resonance at 153.11 ppm to the [*rrm*] sequence, leaving the remaining [*mmr*] and [*mmm*] tetrads collectively at 153.70 ppm and the negligible [*mrm*] tetrad absent. It is notable that the [*rrm*] resonance in the $^{13}C\{^{1}H\}$ NMR spectrum of isotactic PCHC (Figure 4.9d) is shifted 0.1 ppm upfield from that of syndiotactic PCHC (Figure 4.9a and 4.9b), which we attribute to the minor influence of the long-range polymer tacticity on this shift.

To further support the PCHC $^{13}C\{^{1}H\}$ NMR assignments that we propose, we applied Bernoullian statistical methods and compared the observed concentration of each tetrad with its corresponding calculated amount (Scheme 4.2). Table 4.6 compares observed tetrad concentrations to their calculated statistical occurrences for a series of syndiotactic PCHCs. In most cases, the observed and calculated concentrations are in close agreement, and are within the expected error of the deconvolution methods used. Notably, the PCHCs with the highest observed % *r*-centered tetrads overall have relative tetrad concentrations that best agree with the corresponding calculated values.

The $^{13}C\{^{1}H\}$ NMR spectrum of less syndiotactic PCHC, as generated from catalyst **2.3** shows the [*rrr*] and [*rrm*] tetrad resonances approach each other in magnitude with a more significant contribution from the [*mmm*] and [*mmr*] tetrads (Figure 4.8b). Using Bernoullian statistical methods, we calculate relative tetrad occurrences of [*mmm*]/[*mmr*] = 15%, [*rmr*] = 15%, [*rrr*] = 35%, [*rrm*] = 29% and

[*mrm*] = 6% (Table 4.6). This is indeed consistent with what we observe, where a previously minor resonance at 153.18 ppm is now more prominent, which we assign to the [*mrm*] tetrad. In this spectrum we detect fine splitting of various resonances in the 153.2 – 152.9 ppm region, and hypothesize that due to the increase of PCHC stereoerrors we are able to observe signals at greater than tetrad resolution.

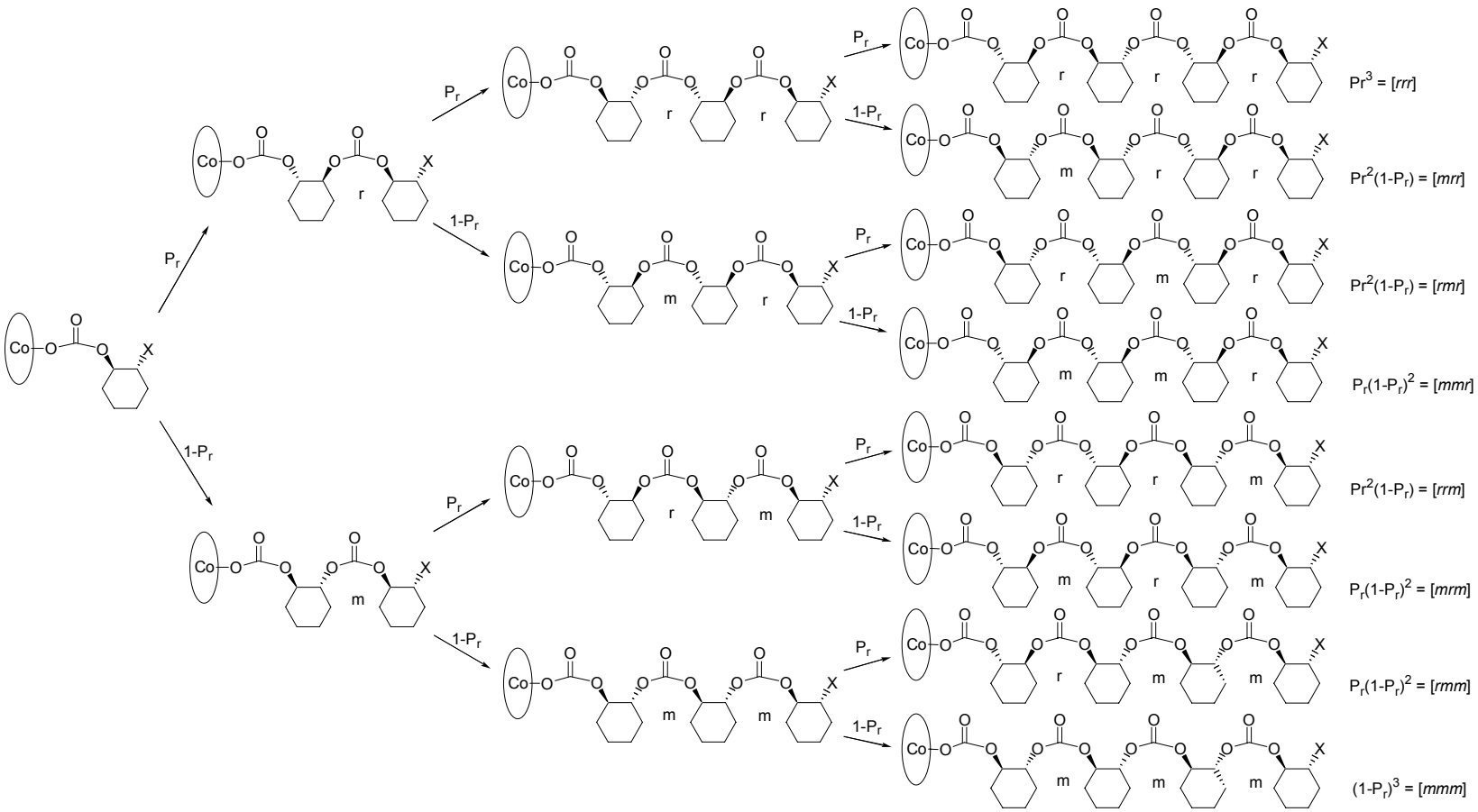

Scheme 4.2. The Bernoullian (chain-end control) expressions in the Bovey formalism (P_r is the probability of a *racemo* diad) for tetrad sequences are the following: [*rrr*] = P_r^3; [*rrm*] = 2[$P_r^2(1\text{-}P_r)$]; [*mrm*] = $P_r(1\text{-}P_r)^2$; [*mmm*] = $(1\text{-}P_r)^3$; [*mmr*] = 2[$P_r(1\text{-}P_r)^2$]; [*rmr*] = $P_r^2(1\text{-}P_r)$.

Furthermore, the $^{13}C\{^{1}H\}$ NMR spectrum of the same PCHC sample using a lower resolution spectrometer showed only the five resonances at 152.95, 153.06, 153.12, 153.17, and 153.70 ppm.

The $^{13}C\{^{1}H\}$ NMR spectrum of PCHC, as generated from catalyst **4.9**, reveals that the [*mmm*]/[*mmr*] tetrads integrate equally to those of the remaining tetrads, indicative of the formation of atactic polymer (Figure 4.9c). Finally, isoenriched PCHC, as generated from catalyst **2.29** while carrying out the CHO/CO_2 copolymerization at low CO_2 pressures (100 psi) has a $^{13}C\{^{1}H\}$ NMR spectrum similar to that of previously reported isotactic PCHC.[4, 6] In this case we observe a large resonance correlating to the combined [*mmm*]/[*mmr*] tetrads at 153.70 ppm and additional resonances representing the [*rrm*] and [*mrm*] stereoerrors with no detectable [*rrr*] or [*rmr*] tetrads (Figure 4.9d).

The methylene regions in the PCHC $^{13}C\{^{1}H\}$ NMR spectra also vary with PCHC stereochemistry (Figure 4.10). In the case of syndiotactic PCHC, two series of two adjacent resonances are observed which we assign to the [*rr*] and [*mr*] triads corresponding to the non-equivalent methylene carbons in the PCHC backbone (Figure 4.10a). In each case, the [*mr*] and [*rm*] triad resonances cannot be distinguished. Furthermore, we suspect that one of these two triads has the same $^{13}C\{^{1}H\}$ NMR shift as the [*rr*] triad. The $^{13}C\{^{1}H\}$ NMR spectrum of less syndiotactic PCHC shows [*rr*] triads of decreased intensity relative to the [*mr*] triad resonances and additional downfield resonances are detected which we assign to the [*mm*] triads (Figure 4.10b). Alternatively, the $^{13}C\{^{1}H\}$ NMR spectrum of atactic PCHC reveals more intense [*mm*] triad resonances compared to the syndiotactic PCHC samples, with the [*mr*] and [*rr*] triad resonances also present (Figure 4.10c). In this case, we observe some tetrad resolution where the [*rr*] triad resonances are split into their [*rrm*] and [*rrr*] components and the [*mr*] triad resonances are broadened. Finally, the $^{13}C\{^{1}H\}$

NMR spectrum of isoenriched PCHC shows that the downfield [*mm*] triad resonances in the methylene region have the greatest intensities relative to the [*mr*] and [*rr*] triad signals (Figure 4.10d).

. It has been shown by both Nozaki and coworkers and in our group that isotactic PCHC has a melting point transition (T_m) > 200 °C.[4, 6] Although the PCHCs we prepared are highly syndiotactic, these polymers are amorphous, with no observable T_m (see appendix A1). Furthermore, the possibility of crystalline syndiotactic PCHC may require a higher % *r*-centered tetrads then that of the polymers presented herein. Thus far, attempts to achieve syndiotactic PCHC with fewer stereoerrors using catalyst **4.5** or **4.6** at lower temperatures or with solvent has not yet realized a substantially more syndiotactic PCHC, and further research is currently underway.

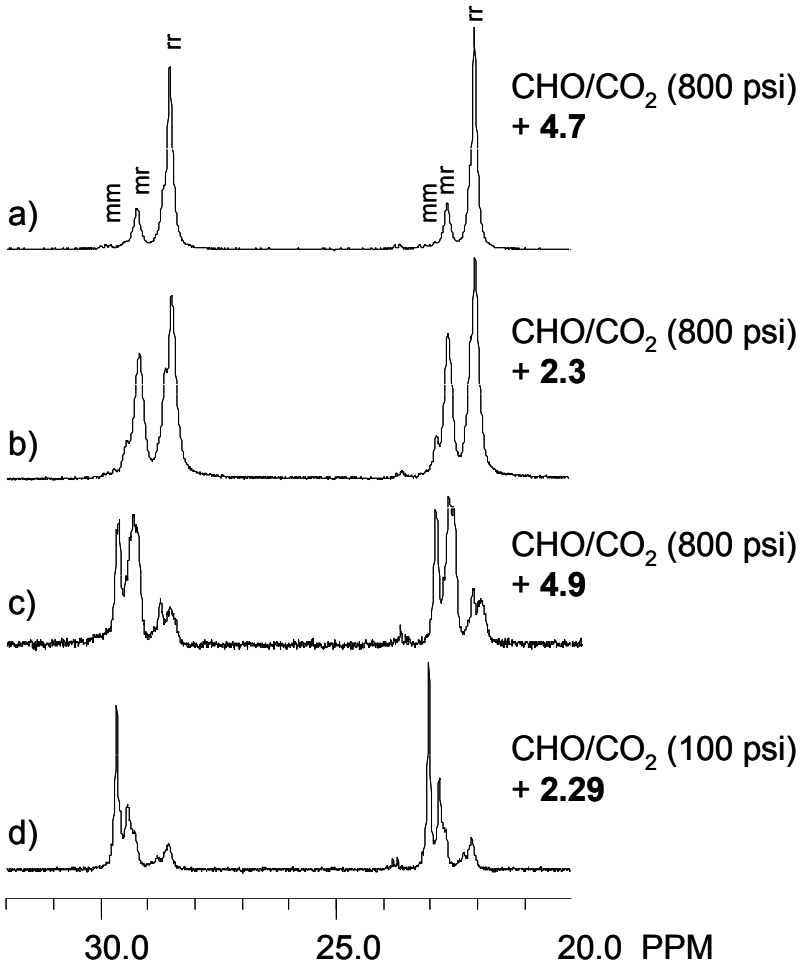

Figure 4.10. Methylene region of the $^{13}C\{^1H\}$ NMR spectra ($CDCl_3$, 125 MHz, d_1 = 10s) of PCHCs generated using CHO/CO_2 (800 psi) with catalyst a) *rac*-(salen-**2**)CoOBzF_5 (**4.7**), b) (*R,R*)-(salen-**1**)CoOBzF_5 (**2.3**), c) *rac*-(salen-**13**)CoOBzF_5 (**4.9**) and d) CHO/CO_2 (100 psi) with catalyst (*R,R*)-(salen-**11**)CoBr (**2.29**).

4.9 Conclusions

We have explored a series of (salen)CoX catalysts for the alternating copolymerization of CHO and CO_2. These catalysts provide a viable route to syndiotactic PCHC, a previously unreported PCHC microstructure. The structural properties of the salen ligands supporting these catalysts dictate the syndiotacticity of the resultant PCHC, a correlation which we attribute to a competition of chain-end and enantiomorphic-site control mechanisms. Additionally, catalyst syndioselectivity is pressure dependent, with the best selectivity realized employing high CO_2 pressures. PCHC with as high as 81% *r*-centered tetrads was obtained using this class of catalyst. Inclusion of [PPN]Cl cocatalysts to the (salen)CoX catalyzed CHO/CO_2 copolymerization results in an increase in catalyst activity in most cases with an overall loss in syndioselectivity. Under optimized conditions, these systems achieve a TOF of 440 h^{-1} for the generation of atactic PCHC.

4.10 Experimental section

4.10.1 General procedures

All air or water sensitive reactions were carried out under dry nitrogen using an MBraun Labmaster drybox or standard Schlenk-line techniques. Methylene chloride and diethyl ether were dried and degassed by passing through a column of activated alumina and by sparging with dry nitrogen. (*S,S*)- and (*R,R*)-*N,N′*-bis(3,5-di-*tert*-butylsalicylidene)-1,2-diaminocyclohexane cobalt(II) ((*S,S*)-(salen-**1**)Co^{II} and (*R,R*)-(salen-**1**)Co^{II}) were purchased from Aldrich and recrystallized from methylene chloride and methanol. Bis(triphenylphosphine)iminium chloride ([PPN]Cl) was purchased from Strem and recrystalized from dry methylene chloride and diethyl ether under nitrogen before use. CHO was dried over calcium hydride and vacuum transferred before use. CO_2 (99.998% purity) was purchased from Airgas and passed over a column of 4Å molecular sieves. All other reagents were purchased from

commercial sources and used as received. Varian Mercury (^{1}H NMR, 300 MHz) and Varian Inova (^{1}H NMR, 500 MHz; ^{13}C{^{1}H} NMR, 125 MHz; ^{19}F NMR, 470 MHz) spectrometers were used to record ^{13}C{^{1}H}, ^{19}F, and ^{1}H NMR spectra, which were referenced versus residual nondeuterated solvent shifts. C_6F_6 (–162.90 ppm) was used as a reference for all ^{19}F NMR spectra. Quantitative ^{13}C{^{1}H} NMR spectroscopy ($CDCl_3$, 125 MHz, d_1 = 10s) was used for integration of the carbonyl region of PCHC (t_1 = 2.0s). GPC analyses were carried out using a Waters instrument (M515 pump, U6K injector) equipped with Waters UV486 and Waters 2410 detectors, and four 5-μm PL Gel columns (Polymer Laboratories; 100 Å, 500 Å, 1000 Å, and Mixed C porosities) in series. The GPC columns were eluted with THF at 40 ºC at 1 mL/min and were calibrated using 23 monodisperse polystyrene standards. IR spectra were measured on a Mattson Research Series FTIR. High resolution mass spectra were obtained from the Mass Spectrometry Laboratory, School of Chemical Sciences, University of Illinois. All (salen)CoX (X = Br or $OBzF_5$) complexes reveal axial ligand (X) loss in the (EI) mass spectra attributable to the poor stability of this complex under the applied conditions. In the case of all (salen)$CoOBzF_5$ complexes, carbons on the phenyl group of pentafluorobenzoate were not assigned in the ^{13}C NMR spectra due to complex carbon fluorine splitting patterns.

4.10.2 Synthesis of ligand precursors

The synthetic procedures for (*R,R*)-(salen-**1**)H_2 (**2.6**), *rac*-(salen-**1**)H_2 (**2.7**), (salen-**3**)H_2 (**2.9**), (salen-**4**)H_2 (**2.10**), (*R,R*)-(salen-**5**)H_2 (**2.11**), (salen-**6**)H_2 (**2.12**), and (*R,R*)-(salen-**11**)H_2 (**2.17**) have been previously described in Chapter 2. The analytical data and synthetic modifications for additional salen ligands are listed below:

***rac*-(Salen-2)H_2 (4.1, CTC-5-22).** To a stirring solution of 3,5-di-tert-butyl-4-hydroxybezaldehyde (3.00 g, 12.8 mmol) in ethyl alcohol (75 mL) open to air was added 1-methylenediamine (0.55 mL, 6.4 mmol) and the solution was heated at reflux

for 12 h. The reaction mixture was cooled to –20 °C, and then filtered and washed with cold ethyl alcohol to afford yellow crystals (2.8 g, 87%) which was in agreement with literature characterization.[18]

***rac*-(Salen-12)H_2 (4.2, CTC-5-119).** 3,5-Bis(α,α'-dimethylbenzyl)-2-hydroxybenzaldehyde[28] (0.59 g, 1.6 mmol), 1,2-diaminopropane (68 μL, 0.80 mmol) and ethyl alcohol (10 mL) were mixed and the reaction was heated at reflux for 12 h. The reaction was cooled to 22 °C, and the solvent was removed *in vacuo*. Following recrystallization from ethyl alcohol, the product was collected as yellow needles (0.41 g, 68%). ^{1}H NMR ($CDCl_3$, 500 MHz): δ 1.25 (d, ^3J = 4 Hz, 3H), 1.595 (s, 3H), 1.599 (s, 3H), 1.61 (s, 3H), 1.62 (s, 3H), 1.698 (s, 3H), 1.702 (s, 3H), 3.58 - 3.75 (m, 3H), 7.13-7.32 (m, 24H), 8.23 (s, 1H), 8.27 (s, 1H), 13.34 (broad s, 2H). ^{13}C{^{1}H} NMR ($CDCl_3$, 125 MHz): δ 20.56, 29.29, 29.73, 29.92, 31.05, 31.06, 31.08, 42.27, 42.31, 42.54, 65.08, 65.80, 118.01, 125.17, 125.70, 125.73, 125.76, 126.84, 127.91, 127.98, 127.15, 129.34, 136.00, 136.17, 139.62, 139.69, 150.71, 150.84, 150.85, 157.69, 157.88, 165.17, 166.97. HRMS (ESI) *m/z* calcd ($C_{53}H_{58}N_2O_2$ + H^+) 755.4577 found 755.4571.

***rac*-(Salen-13)H_2 (4.3, CTC-5-12).** 2-Hydroxy-3-methylbenzaldehyde (0.50 g, 3.7 mmol), 1,2-diaminopropane (0.16 mL, 1.9 mmol), and ethyl alcohol (10 mL) were used, and the reaction was refluxed for 12 h. Following the removal of solvent *in vacuo*, the crude yellow oil was used for the synthesis of *rac*-(salen-**8**)Co without further purification. ^{1}H NMR ($CDCl_3$, 500 MHz): δ 1.38 (d, ^3J = 5 Hz, 3H), 2.23 (s, 3H), 2.24 (s, 3H), 3.69 (m, 2H), 3.83 (m, 1H), 6.74 (t, ^3J = 7.5 Hz, 1H), 6.75 (t, ^3J = 7.5 Hz, 1H), 7.05 (d, ^3J = 7.5 Hz, 2H), 7.14 (d, ^3J = 7.5 Hz, 2H), 8.29 (s, 1H), 8.33 (s, 1H), 13.52 (broad s, 2H).

***rac*-(Salen-14)H_2 (4.4, CTC-5-56).** 3-*tert*-Butyl-2-hydroxybenzaldehyde (1.0 mL, 5.4 mmol), 1,2-diaminopropane (0.23 mL, 2.7 mmol), and ethyl alcohol (10 mL)

were used, and the mixture was refluxed for 12 h. Following the removal of solvent *in vacuo*, the crude yellow oil was used for the synthesis of *rac*-(salen-**9**)Co without further purification. ^{1}H NMR ($CDCl_3$, 500 MHz): δ 1.42 (s, 9H), 1.43 (s, 9H), 1.44 (m, 3H), 3.70 – 3.75 (m, 2H), 3.82 – 3.87 (m, 1H), 6.78 (t, ^3J = 7.5 Hz, 2H), 7.08 (d, ^3J = 7.5 Hz, 2H), 7.30 (d, ^3J = 7.5 Hz, 2H), 8.34 (s, 1H), 8.38 (s, 1H), 13.79 (broad s, 2H).

***rac*-(Salen-15)H_2 (4.5, CTC-5-137).** 5-Bromo-3-*tert*-butyl-2-hydroxybenzaldehyde[29] (0.20 g, 0.78 mmol), 1,2-diaminopropane (33 μL, 0.39 mmol), and ethyl alcohol (10 mL) were used, and the reaction was refluxed for 12 h. Following the removal of solvent, the crude yellow solid was dried *in vacuo* (0.20 g, 93%). ^{1}H NMR ($CDCl_3$, 500 MHz): δ 1.40 (s, 9H), 1.41 (s, 9H), 1.44 (m, 3H), 3.68 - 3.74 (m, 2H), 3.85 - 3.86 (m, 1H), 7.19 (s, 2H), 7.37 (s, 2H), 8.24 (s, 1H), 8.27 (s, 1H), 13.84 (s, 2H). ^{13}C{^{1}H} NMR ($CDCl_3$, 125 MHz): δ 20.46, 29.28, 29.33, 35.26, 35.28, 64.92, 65.54, 109.98, 110.02, 119.91, 131.81, 131.88, 132.62, 132.69, 140.21, 140.33, 159.56, 159.69, 164.39, 166.17. HRMS (ESI) *m/z* calcd ($C_{25}H_{32}Br_2N_2O_2$ + H^+) 551.0909, found 551.0910.

4.10.3 Synthesis of (salen)Co^{II} precursors

The preparation of complexes (*R,R*)-(salen-**1**)Co^{II}, *rac*-(salen-**1**)Co^{II}, (salen-**3**)Co^{II} (**2.9**), (salen-**4**)Co^{II}, (*R,R*)-(salen-**5**)Co^{II}, (salen-**6**)Co^{II}, and (*R,R*)-(salen-**11**)Co^{II} have been described previously in Chapter 2. All other (salen)Co^{II} complexes are described below:

***rac*-(Salen-2)Co^{II} (CTC-5-24).** *rac*-(Salen-**2**)H_2 (2.8 g, 5.5 mmol) and cobalt acetate tetrahydrate (1.7 g, 6.7 mmol) were added to a Schlenk flask charged with a Teflon stir bar under N_2. A 1:1 mixture of toluene and methanol (150 mL, degassed for 20 min by sparging with dry N_2) was added and stirred at 22 °C for 6 h. The

resultant red precipitate was filtered in air and washed with distilled water (50 mL) and methanol (50 mL) and collected as a crude solid (3.0 g, 95% yield).

***rac*-(Salen-12)Co^{II} (CTC-5-123).** Employing the same reaction conditions as for *rac*-(salen-**2**)Co^{II}, *rac*-(salen-**12**)H_2 (0.30 g, 0.40 mmol) and cobalt acetate tetrahydrate (0.12 g, 0.48 mmol) in a 1:1 mixture of degassed toluene and methanol (10 mL) were stirred for 3 h to afford a crude red solid (0.25 g, 77%). IR (KBr, cm^{-1}) 765, 777, 787, 818, 873, 957, 1031, 1106, 1166, 1226, 1323, 1370, 1427, 1441, 1497, 1526, 1583, 1607, 2904, 2926, 2966, 3060. HRMS (ESI) *m/z* calcd ($C_{53}H_{56}CoN_2O_2$) 811.3674, found 811.3698.

***rac*-(Salen-13)Co^{II} (CTC-5-16).** Employing the same reaction conditions as for *rac*-(salen-**2**)Co^{II}, the crude yellow oil *rac*-(salen-**13**)H_2 (2.1 g, 6.8 mmol) was dissolved in a 1:1 mixture of degassed toluene and methanol (40 mL), and cobalt acetate tetrahydrate (2.0 g, 8.0 mmol) were stirred for 1 h to afford a crude red-brown solid (1.95 g, 78%). IR (KBr, cm^{-1}) 739, 888, 947, 1106, 1120, 1234, 1318, 1376, 1419, 1451, 1545, 1604, 2920, 2966, 3020, 3439. HRMS (ESI) *m/z* calcd ($C_{19}H_{20}CoN_2O_2$) 367.0857, found 367.0843.

***rac*-(Salen-14)Co^{II} (CTC-5-64).** Employing the same reaction conditions as for *rac*-(salen-**2**)Co^{II}, the crude yellow oil *rac*-(salen-**14**)H_2 (2.2 g, 5.6 mmol) was dissolved in a 1:1 mixture of degassed toluene and methanol (40 mL), and cobalt acetate tetrahydrate (1.6 g, 6.4 mmol) were stirred for 3 h to afford a crude red solid (1.4 g, 55%). IR (KBr, cm^{-1}) 753, 869, 886, 952, 1057, 1086, 1147, 1200, 1235, 1266, 1316, 1386, 1408, 1466, 1535, 1597, 2873, 2921, 2953. HRMS (ESI) *m/z* calcd ($C_{25}H_{32}CoN_2O_2$) 451.1796, found 451.1776.

***rac*-(Salen-15)Co^{II} (CTC-5-120 and CTC-141).** Employing the same reaction conditions as for *rac*-(salen-**2**)Co^{II}, *rac*-(salen-**15**)H_2 (0.22 g, 0.40 mmol) and cobalt acetate tetrahydrate (0.12 g, 0.48 mmol) in a 1:1 mixture of degassed toluene and

methanol (7 mL) were stirred for 2 h to afford a crude red solid (0.10 g, 41%). IR (KBr, cm^{-1}) 734, 783, 865, 1179, 1310, 1385, 1402, 1525, 1592, 2873, 2922, 2957. HRMS (ESI) *m/z* calcd ($C_{25}H_{30}Br_2CoN_2O_2$) 607.0006, found 607.0010.

4.10.4 Synthesis of (salen)CoX (X = Cl, Br, I, OAc, $OBzF_5$) complexes

The synthesis of (*R,R*)-(salen-**1**)CoX (X = Cl (**2.4**), Br (**2.5**), I (**2.2**), OAc (**2.1**), $OBzF_5$ (**2.3**)), *rac*-(salen-**1**)CoBr (**2.30**), (salen-**3**)CoBr (**2.20**), (salen-**4**)CoBr (**2.19**), (*R,R*)-(salen-**5**)CoBr (**2.22**), (salen-**6**)CoBr (**2.23**), (*R,R*)-(salen-**11**)CoBr (**2.29**), (*R,R*)-(salen-**11**)$CoOBzF_5$ (**3.7**), and (*R,R*)-(salen-**5**)$CoOBzF_5$ (**3.5**) have been described previously in chapters 2 and 3. A modified procedure as reported by Jacobsen and coworkers[30] for the synthesis of **2.4** was applied to the synthesis of all (salen)CoBr complexes with the substitution of NaBr for NaCl. All other (salen)CoX complexes are described below:

***rac*-(Salen-2)CoBr (4.6, CTC-5-32).** *rac*-(Salen-**2**)Co^{II} (1.0 g, 1.8 mmol) and *p*-toluenesulfonic acid monohydrate (0.34 g, 1.8 mmol) were added to a 50 mL round-bottomed flask charged with a Teflon stir bar. Methylene chloride (30 mL) was added to the reaction mixture and stirred for 2 h open to air at 22 °C. The solvent was removed by rotary evaporation at 22 °C, and the crude dark green solid was dissolved in pentane (50 mL) and filtered. The solvent was removed by rotary evaporation, and the material was dissolved in methylene chloride (50 mL) and added to a 250 mL separatory funnel. The organic layer was shaken vigorously with saturated aqueous NaBr (3 x 50 mL). The organic layer was dried over Na_2SO_4 and evaporated under reduced pressure. The solid was suspended in pentane and filtered to afford *rac*-(salen-2)CoBr (0.50 g, 43%). ^{1}H NMR (DMSO-d_6, 500 MHz): δ 1.30 (s, 18H), 1.61 (d, ^3J = 6.5 Hz, 3H), 1.73 (s, 18H), 3.86 (m, 1H), 4.21 (m, 1H), 4.32 (m, 1H), 7.33 (d, ^4J = 2.0 Hz, 1H), 7.40 (d, ^4J = 2.0 Hz, 1H), 7.44 (s, 1H), 7.45 (s, 1H), 7.93 (s, 1H), 8.09 (s, 1H). $^{13}C\{^1H\}$ NMR (DMSO-d_6, 125 MHz): δ 18.45, 30.34, 30.38, 31.51, 31.54,

33.39, 33.43, 35.71, 35.73, 62.99, 64.57, 118.57, 118.88, 128.15, 128.67, 128.74, 128.82, 135.84, 136.01, 141.73, 142.01, 161.67, 161.94, 167.03, 168.55. HRMS (EI) *m/z* calcd. ($C_{33}H_{48}BrCoN_2O_2$ – Br) 563.3048, found 563.3037.

***rac*-(Salen-2)CoOBzF$_5$ (4.7, CTC-5-133).** To a 50 mL round-bottomed flask charged with a Teflon stir bar was added *rac*-(salen-**2**)Co^{II} (0.50 g, 0.89 mmol), pentafluorobenzoic acid (0.19 g, 0.89 mmol) and methylene chloride (10 mL). The mixture was stirred open to air for 12 h at 22 °C. The methylene chloride was removed by rotary evaporation, and the crude solid was dissolved in toluene and filtered. The toluene was then evaporated, and the green solid was washed with pentane (50 mL) and filtered. Drying *in vacuo* afforded a green solid (0.32 g, 46%). ^{1}H NMR (DMSO-d_6, 500 MHz): δ 1.297 (s, 9H), 1.301 (s, 9H), 1.61 (d, ^3J = 6.0 Hz, 3H), 1.727 (s, 9H), 1.735 (s, 9H), 3.86 (dd, ^2J = 12.5 Hz, ^3J = 6.0 Hz, 1H), 4.21 (dd, ^2J = 12.5 Hz, ^3J = 6.0 Hz, 1H), 4.32 (m, 1H), 7.33 (s, 1H), 7.40 (s, 1H), 7.45 (s, 2H), 7.93 (s, 1H), 8.09 (s, 1H). ^{13}C{^{1}H} NMR (DMSO-d_6, 125 MHz): δ 18.47, 30.36, 31.52, 33.43, 35.76, 63.05, 64.66, 118.58, 118.90, 128.20, 128.86, 136.17, 141.79, 142.04, 162.15, 167.13, 168.60. ^{19}F NMR (DMSO-d_6, 470 MHz): δ -163.53, -162.90, -144.86. HRMS (EI) *m/z* calcd ($C_{40}H_{48}CoF_5N_2O_4$ – $C_7F_5O_2$) 563.3048, found 563.3042.

***rac*-(Salen-12)CoOBzF$_5$ (4.8, CTC-5-126).** To a 50 mL round-bottomed flask charged with a Teflon stirbar was added *rac*-(salen-**12**)Co^{II} (0.20 g, 0.25 mmol), pentafluorobenzoic acid (53 mg, 0.25 mmol) and toluene (10 mL). The mixture was stirred open to air for 12 h at 22 °C. The toluene was removed by rotary evaporation and the crude solid was washed with pentane (100 mL), filtered, and dried *in vacuo* to afford a green solid (0.13 g, 51%). ^{1}H NMR ($CDCl_3$, 500 MHz): δ 1.48 (d, ^3J = 6.0 Hz, 3H), 1.57 (s, 6H), 1.58 (s, 6H), 1.93 (s, 3H), 2.02 (s, 3H), 2.05 (s, 3H), 2.07 (s, 3H), 3.68 (dd, ^2J = 13.0 Hz, ^{3}J = 6.0 Hz, 1H), 4.01 (dd, ^2J = 13.0 Hz, ^3J = 6.0 Hz, 1H), 4.15 (m, 1H), 6.98 (s, 1H), 7.04 (s, 1H), 7.14 - 7.07 (m, 2H), 7.16 – 7.30 (m, 18H),

7.34 (s, 2H), 7.91 (s, 1H), 8.04 (s, 1H). $^{13}C\{^{1}H\}$ NMR ($CDCl_3$, 125 MHz): δ 18.48, 29.87, 30.12, 30.33, 30.80, 41.37, 41.39, 43.29, 43.40, 62.91, 64.40, 118.58, 119.13, 125.11, 125.38, 125.43, 126.14, 126.19, 126.22, 127.78, 127.90, 129.97, 130.59, 132.89, 133.29, 135.11, 135.36, 140.95, 141.24, 150.57, 150.61, 151.12, 151.21, 161.69, 161.96, 167.52, 168.82. ^{19}F NMR (DMSO-d_6, 470 MHz): δ -163.73, -162.97, -144.96. HRMS (EI) *m/z* calcd ($C_{60}H_{56}CoF_5N_2O_4 - C_7F_5O_2$) 811.3674, found 811.3683.

***rac*-(Salen-13)CoOBzF$_5$ (4.9, CTC-5-89).** Employing the same reaction conditions as for **4.8**, *rac*-(salen-**13**)Co^{II} (0.70 g, 1.9 mmol) and pentafluorobenzoic acid (0.40 g, 1.9 mmol) were used to afford the crude brown product (1.0 g, 91%). ^{1}H NMR ($CDCl_3$, 500 MHz): δ 1.55 (d, ^{3}J = 6.0 Hz, 3H), 2.63 (s, 3H), 2.65 (s, 3H), 3.93 (dd, ^{2}J = 14.0 Hz, ^{3}J = 6.0 Hz, 1H), 4.24 (dd, ^{2}J = 14.0 Hz, ^{3}J = 6.0 Hz, 1H), 4.42 (m, 1H), 6.57 (t, ^{3}J = 7.5 Hz, 2H), 7.32 (d, ^{3}J = 7.5 Hz, 1H), 7.33 (d, ^{3}J = 7.5 Hz, 1H), 7.36 (d, ^{3}J = 7.5 Hz, 1H), 7.41 (d, ^{3}J = 7.5 Hz, 1H), 8.17 (s, 1H), 8.27 (s, 1H). $^{13}C\{^{1}H\}$ NMR ($CDCl_3$, 125 MHz): δ 16.98, 18.81, 63.11, 64.62, 114.48, 114.62, 117.62, 118.07, 130.53, 130.81, 132.02, 132.56, 134.25, 134.34, 162.96, 163.34, 166.90, 168.20. ^{19}F NMR (DMSO-d_6, 470 MHz): δ -163.25, -162.42, -144.35. HRMS (EI) *m/z* calcd. ($C_{26}H_{20}CoF_5N_2O_4$ - $C_7F_5O_2$) 367.0857, found 367.0845.

***rac*-(Salen-14)CoOBzF$_5$ (4.10, CTC-5-90).** Employing the same reaction conditions as for **4.8**, *rac*-(salen-**14**)Co^{II} (0.42 g, 0.92 mmol) and pentafluorobenzoic acid (0.20 g, 0.92 mmol) were stirred for 3 h to afford the crude brown product (0.49 g, 80%). ^{1}H NMR ($CDCl_3$, 500 MHz): δ 1.61 (d, ^{3}J = 6.0 Hz, 3H), 1.73 (s, 18H), 3.89 (dd, ^{2}J = 13.5 Hz, ^{3}J = 6.0 Hz, 1H), 4.23 (dd, ^{2}J = 13.5 Hz, ^{3}J = 6.0 Hz, 1H), 4.36 (m, 1H), 6.59 (t, ^{3}J = 7.5 Hz, 2H), 7.37 – 7.44 (m, 4H), 8.00 (s, 1H), 8.15 (s, 1H). $^{13}C\{^{1}H\}$ NMR ($CDCl_3$, 125 MHz): δ 18.44, 30.11, 35.47, 35.49, 63.16, 64.47, 114.53, 118.98, 119.29, 131.11, 132.94, 133.51, 142.29, 142.52, 163.83, 164.08, 167.00, 168.45. ^{19}F

NMR (DMSO-d_6, 470 MHz): δ -163.27, -162.47, -144.43. HRMS (EI) *m/z* calcd. ($C_{32}H_{32}CoF_5N_2O_4$ - $C_7F_5O_2$) 451.1796, found 451.1776.

***rac*-(Salen-15)CoOBzF$_5$ (4.11, CTC-5-121).** Employing the same reaction conditions as for **4.8**, *rac*-(salen-**15**)Co^{II} (0.10 g, 0.17 mmol) and pentafluorobenzoic acid (36 mg, 0.17 mmol) were stirred for 3 h to afford the crude brown solid (94 mg, 67%). ^{1}H NMR (DMSO-d_6, 500 MHz): δ 1.62 (d, ^3J = 7.0 Hz, 3H), 1.69 (s, 9H), 1.70 (s, 9H), 3.88 (d of d, ^2J = 13.5 Hz, ^3J = 7.0 Hz, 1H), 4.21 (dd, ^2J = 13.5 Hz, ^3J = 7.0 Hz, 1H), 4.34 (m, 1H), 7.37 (d, ^4J = 2.5 Hz, 1H), 7.38 (d, ^4J = 2.5 Hz, 1H), 7.61 (d, ^4J = 2.5 Hz, 1H), 7.69 (d, ^4J = 2.5 Hz, 1H), 8.06 (s, 1H), 8.21 (s, 1H). ^{13}C{^{1}H} NMR ($CDCl_3$, 125 MHz): δ 17.89, 29.54, 29.74, 29.77, 35.67, 35.73, 35.75, 63.40, 64.69, 104.93, 105.00, 120.50, 120.70, 133.51, 133.53, 134.26, 134.82, 145.00, 145.21, 162.87, 163.16, 168.08, 166.61. δ ^{19}F NMR (DMSO-d_6, 470 MHz): δ -163.66, -162.75, -144.89. HRMS (EI) *m/z* calcd. ($C_{32}H_{30}CoF_5N_2O_4$ - $C_7F_5O_2$) 608.9986, found 608.9990.

4.10.5 Representative copolymerization procedure (CTC-5-135). A 100 mL Parr autoclave was heated to 120 °C under vacuum for 4 h, then cooled under vacuum to 22 °C and moved to a drybox. Complex *rac*-(salen-**2**)$CoOBzF_5$ (15.6 mg, 0.0201 mmol), and CHO (1.00 mL, 9.88 mmol) were placed in a glass sleeve with a Teflon stir bar inside the Parr autoclave. The autoclave was pressurized to 800 psi of CO_2 and was left to stir at 22 °C for 3 h. The reactor was vented at 22 °C. A small aliquot of the resultant polymerization mixture was removed from the reactor for ^{1}H NMR and GPC analysis. The remaining polymerization mixture was then dissolved in methylene chloride (5 mL), quenched with 5% HCl solution in methanol (0.2 mL), and precipitated from methanol (30 mL). The polymer was collected and dried *in vacuo* to constant weight, and the polymer yield was determined (0.799 g, 56.9 %).

4.11 References

(1) Coates, G. W. *Chem. Rev.* **2000**, *100*, 1223-1252.

(2) Natta, G.; Pino, P.; Corradini, P.; Danusso, F.; Mantica, E.; Mazzanti, G.; Moraglio, G. *J. Am. Chem. Soc.* **1955**, *77*, 1708-1710.

(3) For reviews on epoxide/CO_2 copolymerizations, see: (a) Ochiai, B.; Endo, T. *Prog. Polym. Sci.* **2005**, *30*, 183 - 215. (b) Moore; D. R.; Coates, G. W. *Angew. Chem. Int. Ed.* **2004**, *43*, 6618 - 6639. (c) Sugimoto H.; Inoue S. *J. Polym. Sci. Polym. Chem.* **2004**, *42*, 5561 - 5573. (d) Darensbourg, D. J.; Mackiewicz, R. M.; Phelps, A. L.; Billodeaux, D. R. *Acc. Chem. Res.* **2004**, *37*, 836 - 844. (e) Darensbourg, D. J.; Holtcamp, M. W. *Coord. Chem. Rev.* **1996**, *153*, 155 - 174. (f) Super, M. S.; Beckman, E. J. *Trends Polym. Sci.* **1997**, *5*, 236 - 240. (g) Kuran, W. *Prog. Polym. Sci.* **1998**, *23*, 919 - 992. (h) Aida, T.; Inoue, S. *Acc. Chem. Res.* **1996**, *29*, 39 - 48.

(4) Nozaki, K.; Nakano, K.; Hiyama, T. *J. Am. Chem. Soc.* **1999**, *121*, 11008-11009.

(5) Nakano, K.; Nozaki, K.; Hiyama, T. *J. Am. Chem. Soc.* **2003**, *125*, 5501-5510.

(6) Cheng, M.; Darling, N. A.; Lobkovsky, E. B.; Coates, G. W. *Chem. Comm.* **2000**, 2007-2008.

(7) Nakano, K.; Hiyama, T.; Nozaki, K. *Chem. Comm.* **2005**, 1871-1873.

(8) Nakano, K.; Kosaka, N.; Hiyama, T.; Nozaki, K. *Dalton Trans.* **2003**, 4039-4050.

(9) Nakano, K.; Nozaki, K.; Hiyama, T. *Macromolecules* **2001**, *34*, 6325-6332.

(10) Qin, Z.; Thomas, C. M.; Lee, S.; Coates, G. W. *Angew. Chem. Int. Ed.* **2003**, *42*, 5484-5487.

(11) Paddock, R. L.; Nguyen, S. T. *Macromolecules* **2005**, *38*, 6251-6253.

(12) Lu, X. B.; Wang, Y. *Angew. Chem. Int. Ed.* **2004**, *43*, 3574-3577.

(13) Darensbourg, D. J.; Mackiewicz, R. M.; Phelps, A. L.; Billodeaux, D. R. *Acc. Chem. Res.* **2004**, *37*, 836-844.

(14) Cheng, M. PhD Dissertation, Cornell University, May **2000**.

(15) Darensbourg, D. J.; Billodeaux, D. R. *Inorg. Chem.* **2005**, *44*, 1433-1442.

(16) Eberhardt, R.; Allmendinger, M.; Rieger, B. *Macromol. Rapid Commun.* **2003**, *24*, 194-196.

(17) (*a*) Darensbourg, D. J.; Mackiewicz, R. M.; Billodeaux, D. R. *Organometallics* **2005**, *24*, 144-148. (*b*) Darensbourg, D. J., Phelps, A. L. *Inorg. Chem.* **2005**, 44, 4622-4629.

(18) Darensbourg, D. J.; Mackiewicz, R. M.; Rodgers, J. L.; Fang, C. C.; Billodeaux, D. R.; Reibenspies, J. H. *Inorg. Chem.* **2004**, *43*, 6024-6034.

(19) Peretti, K. L.; Ajiro, H.; Cohen, C. T.; Lobkovsky, E. B.; Coates, G. W. *J. Am. Chem. Soc.* **2005**, *127*, 11566-11567.

(20) Darensbourg, D. J.; Mackiewicz, R. M.; Rodgers, J. L.; Phelps, A. L. *Inorg. Chem.* **2004**, *43*, 1831-1833.

(21) Aida, T.; Ishikawa, M.; Inoue, S. *Macromolecules* **1986**, *19*, 8-13.

(22) Aida, T.; Inoue, S. *Acc. Chem. Res.* **1996**, *29*, 39-48.

(23) Darensbourg, D. J.; Mackiewicz, R. M. *J. Am. Chem. Soc.* **2005**, *127*, 14026-14038.

(24) Darensbourg, D. J.; Phelps, A. L. *Inorg. Chem.* **2005**, *44*, 4622-4629.

(25) Darensbourg, D. J.; Mackiewicz, R. M.; Billodeaux, D. R. *Organometallics* **2005**, *24*, 144-148.

(26) Following our work, Lu and coworkers published similar studies concerning (salen)CoX catalyzed PO/CO_2 copolymerization: Lu, X. B.; Lei, S.; Wang, Y. M.; Zhang, R.; Zhang, Y. J.; Peng, X. J.; Zhang, Z. C.; Li, B. *J. Am. Chem. Soc.* **2006**, *128*, 1664 - 1674.

(27) Huggins, M. L.; Natta, G.; Desreux, V.; Mark, H. *Pure Appl. Chem.* **1966**, 645-656.

(28) Cherian, A. E.; Lobkovsky, E. B.; Coates, G. W. *Macromolecules* **2005**, *38*, 6259-6268.

(29) Lam, F.; Xu, J. X.; Chan, K. S. *J. Org. Chem* **1996**, *61*, 8414-8418.

(30) Nielsen, L. P. C.; Stevenson, C. P.; Blackmond, D. G.; Jacobsen, E. N. *J. Am. Chem. Soc.* **2004**, *126*, 1360-1362.